OBSERVATIONS OF MERCURY'S EXOSPHERE BY THE MERCURY ATMOSPHERIC AND SURFACE COMPOSITION SPECTROMETER DURING THE FIRST MESSENGER FLYBY: William E. McClintock[1] (william.mcclintock@colorado.edu), E. Todd Bradley[2], Noam R. Izenberg[3], Rosemary M. Killen[4], Mark C. Kochte[3], Mark R. Lankton[1], Nelly Mouawad[4], Ann L. Sprague[5], and Ronald J. Vervack, Jr.[3] [1]LASP, U. Colo., Boulder, CO 80303; [2]University of Central Florida, Department of Physics, Orlando, FL, 32816; [3]JHU/APL, Laurel, MD 20723; [4]University of Maryland, Department of Astronomy, College Park; [5]LPL, U. Arizona, Tucson, AZ 85721.

Introduction: During the first MESSENGER [1] flyby of Mercury, the UltraViolet and Visible Spectrometer (UVVS) channel of the Mercury Atmospheric and Surface Composition Spectrometer [2] (MASCS) will observe Mercury's sodium tail [3] and exosphere. Flybys of the planet provide opportunities for extended tail observations that are precluded during the orbital phase of the MESSENGER mission by spacecraft pointing constraints. Brief observations of the dayside and nightside exosphere near the planet (within a few hundred km of the surface) and of the dayside exosphere out about 10,000 km are also planned for the flybys [4,5,6].

Observations: Figure 1 shows the trajectory of the MESSENGER spacecraft (red line) superimposed on an image of Mercury's Na exosphere and extended tail [3]. Green arrows mark the direction during the inbound leg of the UVVS line of sight (LOS), which is oriented perpendicular to the Sun-planet line. Observations begin when the line of sight crosses the Sun-planet line approximately 24,500 km behind Mercury. Spacecraft rotations articulate the instrument LOS perpendicular to the plane of Figure 1, sweeping out a volume that is approximately three planet diameters tall [5]. The UVVS field of view (FOV) for exosphere observations is 0.04˚ x 1˚, and the spatial resolution of the tail observations varies from ~ 100 x 1000 km (along the Sun-planet line x perpendicular to the Sun-planet line) at the beginning of the measurements to 40 km x 1000 km near the planet.

During this part of the encounter, the UVVS executes alternating grating scans to observe the sodium doublet, located at 589.0/589.6 nm, and the hydrogen Lyman alpha emission, located at 121.6 nm, with a cadence of 30 seconds.

The near-planet portion of the flyby is shown in Figure 2. As MESSENGER passes into the shadow of Mercury, it rotates 180˚ about the Sun line, pointing the remote sensing instruments at the surface. For the next ~ 10 minutes, the UVVS executes scans centered on emission lines of sulfur (186.2 nm), sodium (330.3 nm), calcium (422.7 nm), and potassium (404.7 nm), while the LOS passes through the sunlit exosphere and the FOV intercepts the shadowed surface.

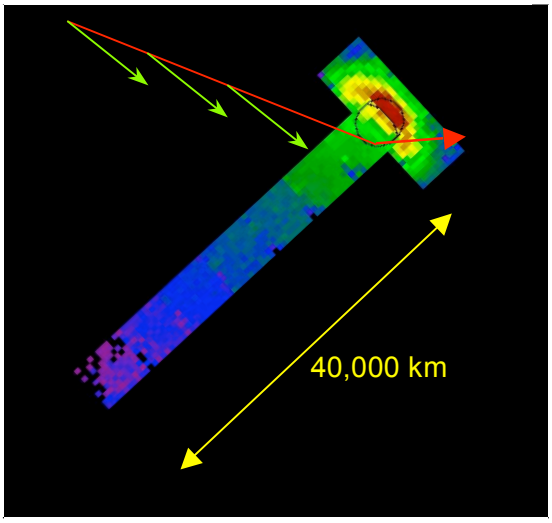

Fig. 1. *The trajectory of the MESSENGER spacecraft (red line) is shown superimposed on an image of Mercury's sodium exosphere and extended antisunward-pointing tail that was obtained on May 26, 2001. Green arrows show the LOS of the UVVS during the flyby approach.*

Vertical lines delineate boundaries of the four MASCS observing sequences. MSCM1 and MSCM2 are tail and nightside exopshere, observations, respectively. MSCS4 marks the region for dayside exosphere measurements. Sunlit surface observations are performed during MSCSM3.

Once the MASCS LOS crosses to the sunlit side of the terminator, the UVVS switches its FOV to 0.04˚ x 0.05˚ and observes the surface using continuous scans that cover 115 – 320 nm in wavelength. As the LOS crosses near the

subsolar point, exosphere observations resume with scans to measure sulfur (181.3 nm) and sodium (589.0/589.6 nm) at low altitudes followed by scans to measure hydrogen, oxygen (130.2 – 130.4 nm), calcium, potassium, and sodium. These continue to an altitude of ~ 10,000 km.

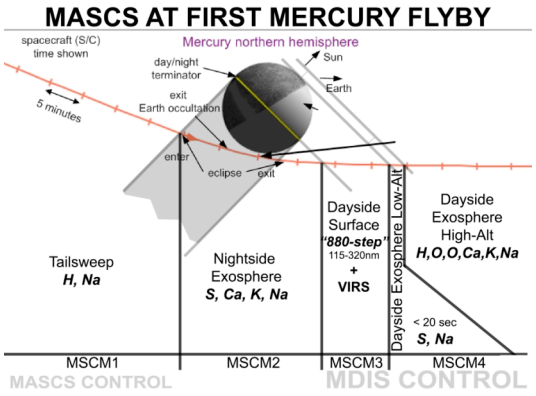

Fig 2. *The orange line shows MESSENGER's trajectory near closest approach during the first Mercury flyby. Ticks mark 5-minute intervals.*

Anticipated Results: The exosphere of Mercury is highly variable, and it is difficult to estimate exospheric emission strengths. The flyby occurs when the Mercury true anomaly is 285°. Ground-based observations of the sodium tail indicate that its emissions will be dimmer and less extended than those shown in Figure 1 [7]. The temporal behavior of other observed species is less well understood. Bradley et al. [5] have estimated detection limits [the emission strength required to produce a signal-to-noise (SNR) of 5 for the various species that the UVVS will scan during the tail and nightside exosphere sequences], and these are summarized in Table 1.

Species	Detection limit (Rayleigh)	Detection limit column abundance (atoms/cm^2)
H	169	2.0 x 10^{10}
O	170	3.2 x 10^{12}
S	1015	2.1 x 10^{12}
Ca	174	7.8 x 10^{6}
K	149	2.0 x 10^{9}
Na (330)	148	2.0 x 10^{9}
Na (589.3)	609	1.0 x 10^{7}

Table 1. Tail and nightside detection limits for SNR = 5, assuming optically thin emissions.

Ground-based observations of Na are often in the 6,000 – 60,000 Rayleighs range, and it would be surprising if MASCS does not return high-quality observations of this species.

Furthermore, the flyby geometry is suited to its measurement in the extended tail. The observing geometry for other species is less favorable, and scattered light from the illuminated surface will raise the detection limits reported in Table 1 when the instrument FOV is close to the planet (< 25° from the sunlit surface). Ca is known to be diffuse and highly variable with emissions of a few hundred Rayleighs [8], and S has not yet been detected, possibly because its resonance lines lie outside the wavelength range accessible by ground-based telescopes.

References: [1] S. C. Solomon *et al.* (2007) *Space Sci. Rev.*, 131, 3-39. [2] W. E. McClintock and M. R. Lankton (2007) *Space Sci. Rev.*, 131, 481-521. [3] A. E. Potter *et al.* (2002) *Meteoritics Planet. Sci.*, 37, 1165-1172. [4] R. M. Killen *et al.* (2008) *Lunar Planet. Sci.*, XXXIX. [5] E. T. Bradley *et al.* (2008) *Lunar Planet. Sci.*, XXXIX. [6] R. J. Vervack, Jr., *et al.* (2008) *Lunar Planet. Sci.*, XXXIX. [7] A. E. Potter *et al.* (2007) *Icarus,* 186, 571-580. [8] R. M. Killen *et al.* (2005) *Icarus* 173, 300-311.